IEICE TRANS. COMMUN., VOL.E103–B, NO.6 JUNE 2020

PAPER

Transmission-Quality-Aware Online Network Design and Provisioning Enabled by Optical Performance Monitoring

Keisuke KAYANO[†], ***Student Member***, **Yojiro MORI**[†a)], ***Member***, **Hiroshi HASEGAWA**[†], ***Senior Member***, **Ken-ichi SATO**[†], ***Fellow, Honorary Member***, **Shoichiro ODA**[††], **Setsuo YOSHIDA**[††], ***Members***, ***and*** **Takeshi HOSHIDA**[††], ***Senior Member***

SUMMARY The spectral efficiency of photonic networks can be enhanced by the use of higher modulation orders and narrower channel bandwidth. Unfortunately, these solutions are precluded by the margins required to offset uncertainties in system performance. Furthermore, as recently highlighted, the disaggregation of optical transport systems increases the required margin. We propose here highly spectrally efficient networks, whose margins are minimized by transmission-quality-aware adaptive modulation-order/channel-bandwidth assignment enabled by optical performance monitoring (OPM). Their effectiveness is confirmed by experiments on 400-Gbps dual-polarization quadrature phase shift keying (DP-QPSK) and 16-ary quadrature amplitude modulation (DP-16QAM) signals with the application of recently developed Q-factor-based OPM. Four-subcarrier 32-Gbaud DP-QPSK signals within 150/162.5/175 GHz and two-subcarrier 32-Gbaud DP-16QAM signals within 75/87.5/100 GHz are experimentally analyzed. Numerical network simulations in conjunction with the experimental results demonstrate that the proposed scheme can drastically improve network spectral efficiency.
key words: *network design, elastic optical network, performance monitoring, higher-order modulation*

1. Introduction

To improve the spectral efficiency of photonic networks, bandwidth-variable transponders (BVTs) are highly effective as they permit the use of higher-order modulation formats and denser wavelength-division multiplexing (WDM) in an adaptive manner [1]–[3]. However, such spectrally efficient systems are susceptible to transmission impairments such as fiber nonlinearity, amplified-spontaneous-emission (ASE) noise, and signal-spectrum narrowing [4], [5]. The distance-adaptive modulation can enhance the spectral efficiency in the presence of fiber nonlinearity and ASE noise by assigning the possible highest modulation order for each optical path [1]. To maximize the spectral efficiency under the influence of signal-spectrum narrowing, both the possible highest modulation order and narrowest channel bandwidth should be assigned to each optical path while meeting the required transmission specifications of paths. However, to accommodate uncertainties in the performance of components including optical fibers, erbium-doped fiber amplifiers (EDFAs), and wavelength-selective switches (WSSs) and to create truly robust systems, network and system design tools have to set sufficient margins as determined by off-line transmission performance analyses. The margins can easily become excessive, i.e. higher than the actually needed margins [7]. Furthermore, the recent trend of optical transport system (OTS) disaggregation forces even greater margins [8]. Presently deployed all-in-one single-vendor network systems use aggregate margins developed from the experiences of system venders and network providers. Disaggregation, however, isolates the margins of the disaggregated parts, which can substantially enlarge the total margin and as a result can increase network cost [7], [9]. In creating reliable and robust networks under such circumstances, excessive margins need to be set to accommodate impairment uncertainties and disaggregation effects, which hinders the use of spectrally efficient modulation formats.

In this paper, we propose transmission-quality-aware online network design and provisioning aiming at margin minimization and spectral-efficiency maximization; the proposal is enabled by a recently developed optical performance monitor (OPM) with Q-factor measurements [10]. Network spectral efficiency is maximized by assigning the possible highest modulation order and narrowest channel bandwidth in accordance with the actually measured performance, since our OPM can precisely assess transmission performance in a path-by-path manner; a benefit not possible with off-line design tools. The measured performance allows the highest possible modulation order and narrowest channel bandwidth to be assigned to each path without excessive margin.

We demonstrate the effectiveness of the proposed scheme by transmission experiments and network simulations for different topologies. First, we measure the Q-factor values of 400-Gbps signals by using our OPM to demonstrate its effectiveness in highly dense WDM networks; we examine four-subcarrier 32-Gbaud dual-polarization quadrature phase shift keying (DP-QPSK) signals within 150/162.5/175 GHz and two-subcarrier 32-Gbaud dual-polarization 16-ary quadrature-amplitude modulation (DP-16QAM) signals within 75/87.5/100 GHz. Second, we execute numerical network simulations in conjunction with the measured results. It is shown that our proposal can drastically improve the spectral efficiency for the tested network topologies. A proof-of-concept evaluation that assumed static-traffic scenarios was reported in [11]. We extend the explanation and discussion

Manuscript received July 8, 2019.
Manuscript revised November 6, 2019.
Manuscript publicized December 4, 2019.
[†]The authors are with Nagoya University, Nagoya-shi, 464-8601 Japan.
[††]The authors are with Fujitsu Limited, Kawasaki-shi, 211-8588 Japan.
a) E-mail: mori@nuee.nagoya-u.ac.jp
DOI: 10.1587/transcom.2019EBP3155

by adding new network simulation results for dynamic traffic scenarios.

The remainder of this paper is organized as follows. Section 2 details our network design proposal based on our recently developed OPM that uses Q-factor measurements. In Sect. 3, we develop a network control algorithm to realize our proposed network while suppressing spectrum fragmentation. Section 4 describes the Q-factor measurements conducted by our OPM, where four-subcarrier 32-Gbaud DP-QPSK signals and two-subcarrier 32-Gbaud DP-16QAM signals are evaluated under different assigned channel bandwidths. Section 5 demonstrates the effectiveness of the proposed network design and provisioning through network simulations, where the modulation order and channel bandwidth are assigned to each path according to the measured results so that the spectral efficiency is maximized. Finally, the paper is concluded in Sect. 6.

2. Transmission-Quality-Aware Network Based on Optical Performance Monitoring

2.1 Margin Minimization by Optical Performance Monitoring with Q-Factor Estimation

Overall margin can be classified into design margin, unallocated margin, and system margin as summarized in Table 1 [6]; the design margin covers the calculation errors of network design tools; the unallocated margin is unintentionally caused by discrete bauds, signal bandwidths, and transmission reaches. The system margin accommodates slowly varying impairments, rapidly varying impairments, and operator's buffer. OTS disaggregation imposes a disaggregation margin [7].

We consider software-defined networks (SDN) in which the route, spectrum, modulation format, and channel bandwidth can be individually controlled by the SDN controller. The information obtained by the OPMs is transferred over the optical supervisory channel [12]. In such systems, the accurate transmission performance measurements yielded by OPM enables precise margin management in a path-by-path manner, and hence the required margin can be minimized. Our recently developed built-in-receiver OPM estimates the Q factor by counting the number of bits corrected in the forward-error-correction (FEC) process [10] and hence the performance of optical-path candidates can be calculated in a fast, accurate, and cost-effective manner. As a result, we can reduce the design margin assigned to handle uncertain transmission impairments and the system margin for slowly varying impairments and disaggregation. The irreducible margins are the system margins for rapidly varying impairments and operator's buffer. This is summarized in the right most column of Table 1.

Table 1 Margin classification.

Margin classification		Origins	Quality-aware network with OPM
Design margin		Calculation errors of design tools	Minimized
Unallocated margin		Discrete data rates, bandwidths, and reaches	Reduced
System margin	Slowly varying impairments	Aging and data loading (nonlinearity)	Minimized
	Fast varying impairments	Polarization impairments etc.	Unchanged
	Disaggregation	Disaggregation of the OTS	Minimized
	Operator's buffer	Extra buffer determined by the operator	Unchanged

2.2 Margin Reduction Using Transmission-Quality-Aware Path Establishment Enabled by Optical Performance Monitoring

The unallocated margin can be reduced by increasing the number of signal form candidates. The distance-adaptive modulation networks that use BVTs [1] adopt the highest-order modulation format possible for the transmission distance of each path. Consequently, the unallocated margin can be reduced and the spectral efficiency is enhanced. To realize reliable distance-adaptive modulation networks, the optical channel guard-band bandwidth must be broad enough so as to avoid the spectrum narrowing caused by WSS traversal; otherwise, an extra margin must be set to accommodate the penalty imposed by the spectrum narrowing. The desirable solution is to assign the modulation order and channel bandwidth according to both the transmission distance and hop count of each path. Figure 1(a) and Fig. 1(b) show the concept of the distance-adaptive method and that of the distance-/hop count-adaptive method, respectively. The distance-adaptive method assigns modulation order according to the distance, whereas the distance-/hop count-adaptive method assigns modulation order and channel bandwidth according to the distance and hop count. The distance-/hop count-adaptive method is expected to attain higher spectral efficiency than the distance-adaptive method. This scheme, however, necessitates extensive analyses of the transmission performance considering all path candidates; a large number of network parameters need to be incorporated and this incurs infeasible computational loads. To realize adaptive control of the modulation order and channel bandwidth in a simple and reliable manner, our OPM utilizes the Q factor. Since the Q factor is calculated by counting the number of recovered bits in the FEC process, precise performance estimation is possible [10]. The measured Q factors allow us to assign the highest modulation order and narrowest channel bandwidth possible for each path while satisfying the Q-factor requirement. It should be noted that OPM based on optical spectrum analyses is not effective when the signal spectrum is narrowed by WSS traversal. The performance monitoring based on the distribution or statistical moments of equalized signals [13]–[15] can include the impacts of spectrum narrowing; however, the estimation error increases

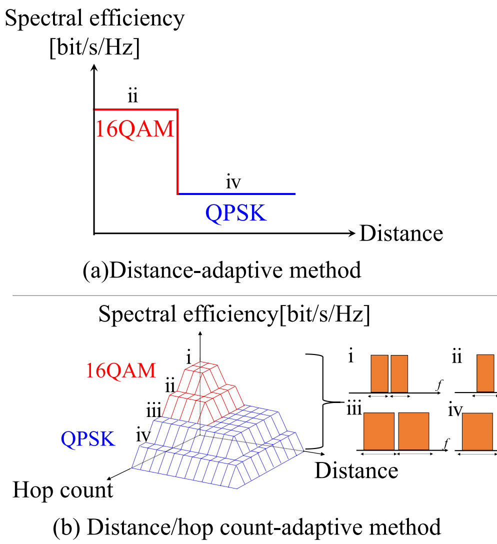

Fig. 1 Concepts of adaptive networking schemes, where the same net bitrate is assumed.

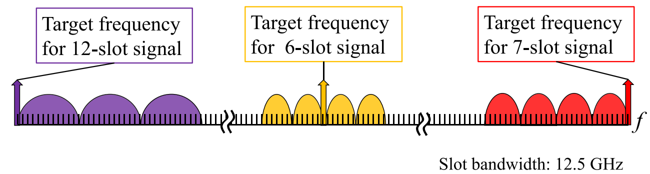

Fig. 2 Example of frequency slot assignment using channel-bandwidth dedicated target frequency strategy.

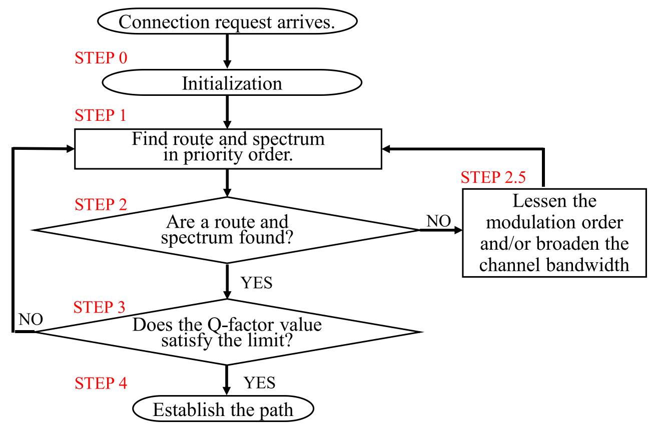

Fig. 3 Flowchart of the path-establishment process.

the margin needed. In contrast, Q factor is an accurate metric of system performance as it encompasses all system impairments and hence precludes the use of excessive margins. The proposed scheme thus can enhance the spectral efficiency without precisely considering each impairment.

3. Network Design and Control Algorithm

3.1 Reduction in Spectrum Fragmentation

An optical path can use multiple frequency slots, but these frequency slots must be consecutively aligned in the frequency domain, which is known as the constraint of spectrum contiguity [17]. In elastic optical networks that utilize many kinds of bandwidths, the constraint yields spectrum fragments that cannot be assigned to any optical path. The spectrum fragmentation is magnified by allowing excessive flexibility in assigning signal spectra. To resolve this issue with spectrum assignment, we adopt a routing and spectrum assignment (RSA) algorithm based on the target-frequency (T-F) spectrum arrangement [16]. Figure 2 provides an example of using the T-F method, where 6-, 7-, and 12-slot channel bandwidths are considered as examples. A target frequency is set for each channel bandwidth. For a newly arriving optical path connection request, the method searches for a frequency slot that is nearest to the target frequency determined for each given channel bandwidth. As a result, paths with the same channel bandwidth are set around the corresponding target frequency and hence the probability of fragmentation is reduced. For further details of the T-F method, refer to [16]. Note that our transmission-quality-aware network scheme can be applied independently of defragmentation algorithms [17]; comparison of the numerous defragmentation schemes is beyond the scope of this paper.

3.2 Network Design and Control Algorithm

Figure 3 depicts the flowchart of the path-establishment process, where the T-F method is applied. The procedure is as follows:

Step 0: Initialization

The highest modulation order and narrowest channel bandwidth are selected as a candidate.

Step 1: Find route and spectrum in order of priority

Find a route and spectrum that can connect the source node and destination node in accordance with the following priority.

1. A route with the shorter hop count
2. A frequency nearer to the target frequency

Step 2: Are the route and spectrum found?

Decide whether the candidate need to be changed.

Step 2.5: Lessen the modulation order and/or broaden the channel bandwidth in accordance with the priority in the list.

The priority list used in this work is indicated in Fig. 8. Block the request if the last candidate on the list fails.

Step 3: Does the Q-factor value satisfy the limit?

Establish the tentative path, measure the Q-factor value of the path using OPM, and judge whether the Q-factor value surpasses the prescribed limit. The limit is determined by the FEC threshold and a set margin.

Step 4: Establish the path.

Establish the path using the assigned route, spectrum, modulation order, and channel bandwidth.

4. Transmission Experiments

4.1 Experimental Setup

As a preliminary for network analyses, we measured Q factors as a function of hop count where the modulation order and channel bandwidth were changed. Figure 4 depicts the network test-bed used for the measurements. We examined the 400-Gbps signal formats recommended by OIF [18], i.e., four-subcarrier 32-Gbaud DP-QPSK signals and two-subcarrier 32-Gbaud DP-16QAM signals. The number of simultaneously loaded wavelength channels was four for the DP-QPSK system and eight for the DP-16QAM system, i.e. 16 subcarriers in both cases. The subcarriers within the signal were aligned with 37.5-GHz spacing. The channel bandwidth was set to 150/162.5/175 GHz for the QPSK signal and 75/87.5/100 GHz for the 16QAM signal; the values conform to the ITU-T flexible grid [19]. The power launched into each fiber was set to 0 dBm per subcarrier. The signals traversed a 40-km single-mode fiber (SMF) followed by variable optical attenuator (VOA); the span loss was set to 15 dB to emulate a transmission distance of 80 km. Here, we consider the network has uniform link length. The signal was delivered to the next node that used an express switch comprised of 1×8 power splitters (PSs) and 8×1 WSSs in broadcast-and-select arrangement. The target-signal spectrum was narrowed with each node traversal. The add/drop parts consisted of multicast switches (MCSs). In the receiver, the digital-signal-processing circuit executed dispersion compensation, polarization demultiplexing, carrier-phase estimation, and FEC. Finally, the OPM derived the Q factor from the number of bits corrected in the FEC process.

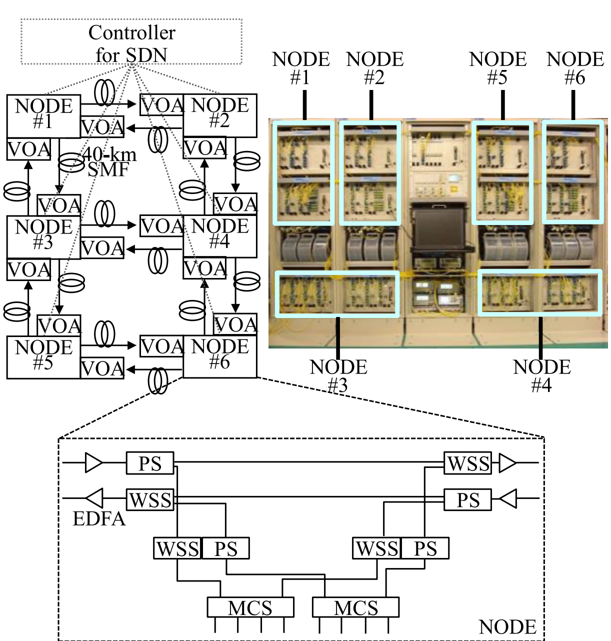

Fig. 4 Network test-bed for the experiment.

4.2 Measured Results

Figure 5 plots the Q factor measured as a function of hop count; the parameters are the assigned modulation order and channel bandwidth. The measured results show that channel bandwidths of 162.5 GHz for the QPSK signal and 87.5 GHz for the 16QAM signal are sufficient to prevent the spectrum-narrowing effect. In contrast, serious signal degradation occurred due to the spectrum-narrowing effect with assigned channel bandwidths of 150 GHz for the QPSK signal and 75 GHz for the 16QAM signal. The maximum assignable hop count depends on both the target Q factor and the necessary margin. For example, if we assume the target Q factor of 5.7 dB and the necessary margin of 2 dB for the 400 Gbps 16-QAM signal, the maximum assignable hop count is 4 for the 75 GHz channel bandwidth and 8 for the 87.5 GHz channel bandwidth.

Figure 6 plots optical signal-to-noise ratio (OSNR)

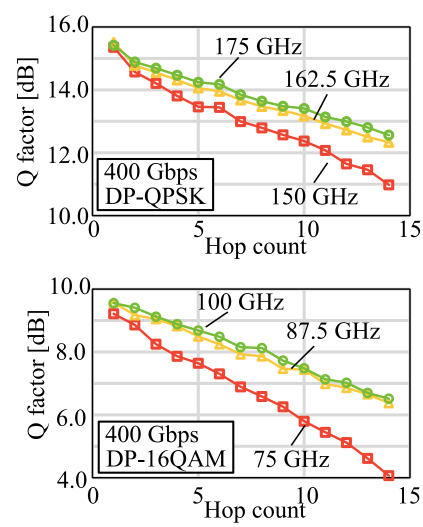

Fig. 5 Q factor measured as a function of hop count.

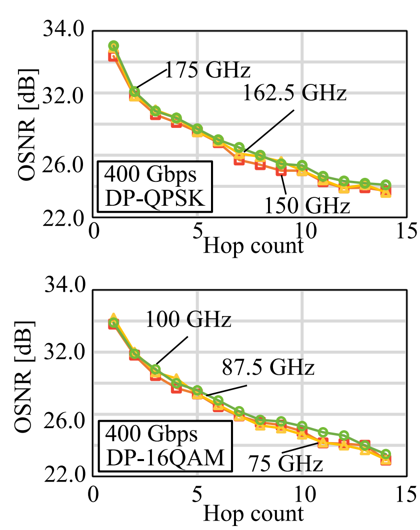

Fig. 6 OSNR measured as a function of hop count.

measured as a function of hop count. Here, we turned off the target signal and measured the noise level at the target frequency by using an optical spectrum analyzer in the typical manner. The noise-level fluctuation due to the signal elimination was less than 0.1 dB. As mentioned above, Q factor can show the signal degradation caused by spectrum narrowing. On the contrary, the OSNR characteristics fail to demonstrate the same degradation, see Fig. 5 and Fig. 6. As is clearly indicated, basing the OPM on OSNR measurement fails to support spectrally efficient systems that exhibit severe spectrum narrowing unless an additional margin is used to fill the gap between Q factor and OSNR. For example, in our tested systems, a 1 dB additional margin would be needed to offset the estimation error of OSNR-based performance monitoring when the modulation order is 400 Gbps DP-QPSK and the hop count is 10. As a result, the spectral efficiency of the network decreases. The effectiveness of our proposed network scheme is thus enhanced by basing the OPM on Q-factor measurements.

In the next section, we show that the spectral efficiency of networks is maximized by appropriately selecting the modulation orders and channel bandwidths indicated by the measured results shown in Fig. 5.

5. Network Simulations

5.1 Simulation Setup

To demonstrate the effectiveness of our network control proposal, three scenarios are investigated using different topology networks assuming dynamic traffic distributions. Scenario A: distance-adaptive network without OPM, Scenario B: distance-adaptive network with OPM, and Scenario C: our proposed transmission-quality-aware network control with OPM. The points of the three networks are summarized in Table 2. The spectrum fragmentation is minimized by the T-F method discussed in Sect. 3.1. We also evaluated the first-fit (F-F) method as a reference. The tested network topologies are illustrated in Fig. 7. All inter-node distances are assumed to be 80 km to match the experimental setup; note that non-uniform inter-node distances are also possible since our OPM can precisely estimate the Q-factor value from the received signal. Path-setup requests are generated in accordance with a Poisson process and the holding time of each connection follows a negative exponential distribution. We assumed that the traffic was uniformly and randomly distributed. The maximum detour from the minimum-hop path route is set to 2 hops. The number of fibers in each link of the network is determined by static network design for each scheme for each assumed traffic demand; the total number of fibers needed in a network for the three scenarios is set to be equal to yield fair comparisons. The available bandwidth of a fiber is 4,400 GHz (i.e. 352 12.5-GHz slots in the C band). We assume the use of 400-Gbps DP-QPSK and DP-16QAM signals as in the experiments. The number of required slots and corresponding bandwidth are summarized in Table 3 and Fig. 8, which are derived by the measured results shown in Fig. 5. Small roman numerals in Fig. 8 represent the assignment priority mentioned in Fig. 3. In Scenario A and B, combinations of modulation order and channel bandwidth are selected out of ii and iv in Fig. 8. In Scenario C, any combination is selectable. As mentioned in Sect. 4.2, the number of slots per channel that can completely avoid the spectrum-narrowing effect are 13 slots (162.5 GHz) in the QPSK system and 7 slots (87.5 GHz) in the 16QAM system. Therefore, 14 slots (175 GHz) in the QPSK system and 8 slots (100 GHz) in the 16QAM system are excluded from the candidates in the scenarios examined.

The Q factor at the FEC threshold is set to 5.7 dB [20]. A 2-dB margin is, as an example, set for the fast-varying impairments and operator's buffer. As for Scenario A, the additional margin of 4 dB (i.e. 6 dB in total) is assumed considering design errors, aging, network loading, and disaggregation. In Scenario B and Scenario C, the margin is

Table 2 Examined network scenarios.

	Scenario A	Scenario B	Scenario C (Proposal)
Transmission analysis	Offline design tools	OPM	OPM
Adaptive assignment	Modulation	Modulation	Modulation & Bandwidth

	British Telecom	Telefonica	Phoenix	6×6
	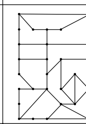	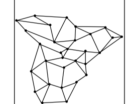	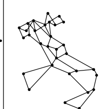	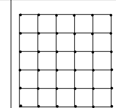
The number of nodes	27	30	31	36
Average hop count	3.43	3.31	3.72	3.95
Maximum hop count	9	9	11	12

Fig. 7 Examined network topologies.

Table 3 Modulation formats and the number of assigned slots.

Modulation format	The number of subcarriers	Scenario A, Scenario B: The number of assigned slots (Slot bandwidth: 12.5 GHz)	Scenario C (Proposal): The number of assigned slots (Slot bandwidth: 12.5 GHz)
32-Gbaud DP-QPSK	4	13	12 or 13
32-Gbaud DP-16QAM	2	7	6 or 7

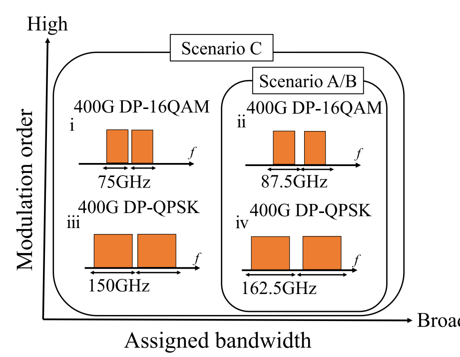

Fig. 8 Network test-bed for the experiment.

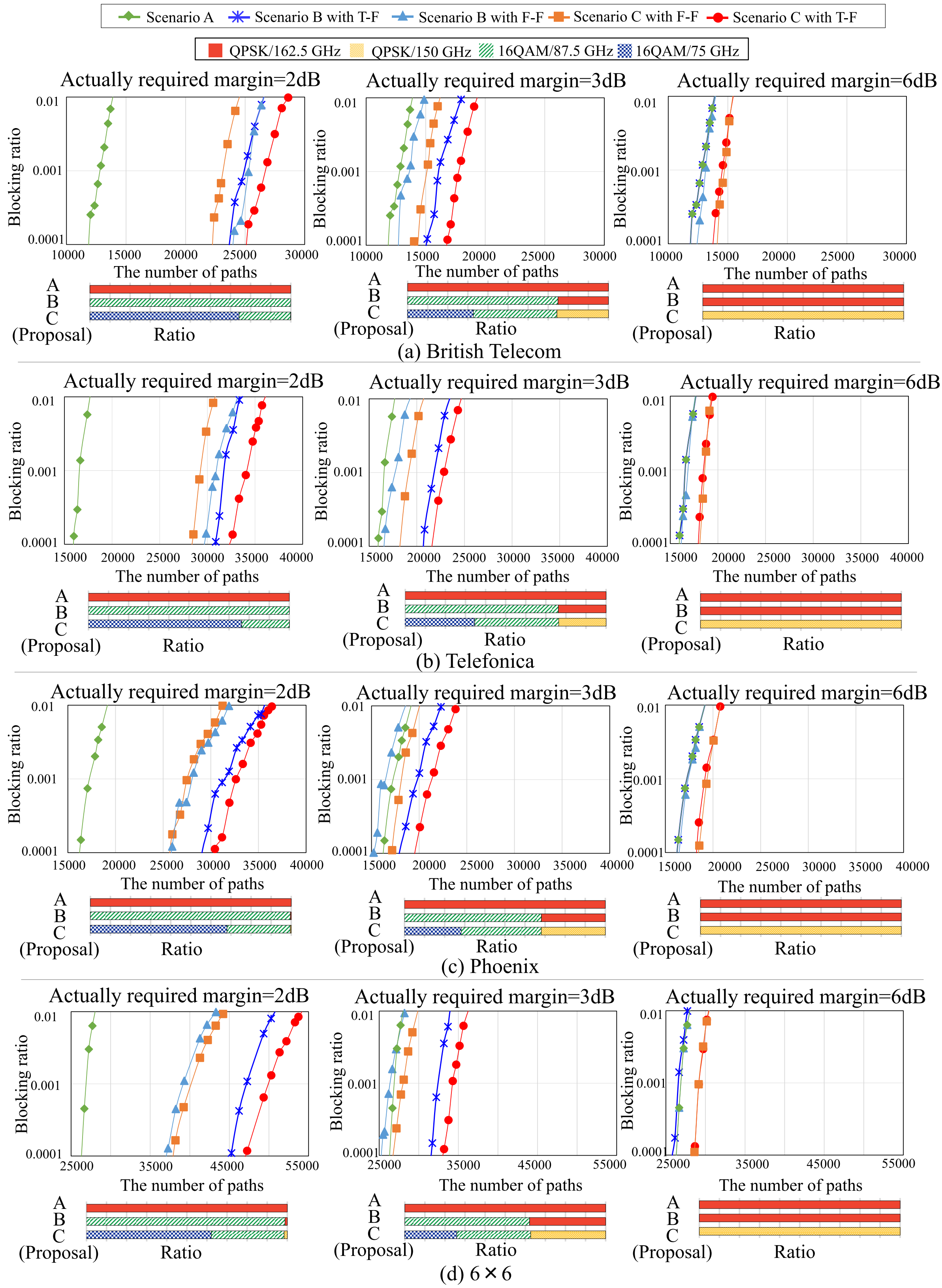

Fig. 9 Blocking ratio versus the number of paths, where the actually required margin is changed. The ratios of assigned modulation orders/channel bandwidths are illustrated. A, B, and C denote the scenarios defined in Sect. 5.1.

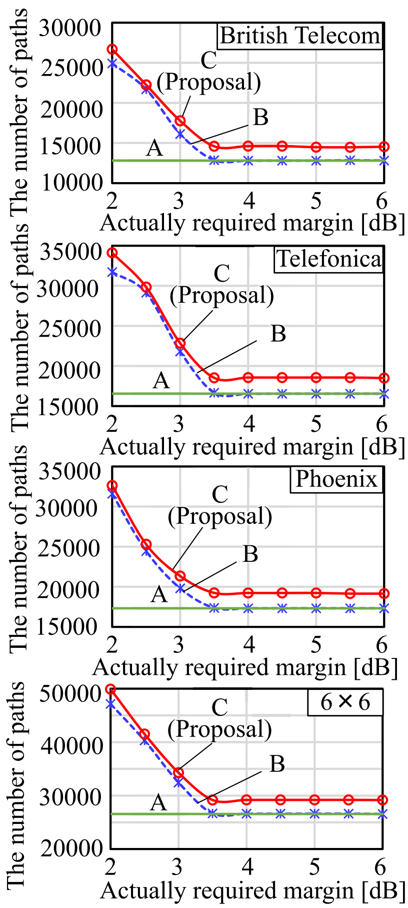

Fig. 10 The number of accommodated paths versus actually required total margin, where the number of accommodated paths is given by the value at the blocking ratio of 10^{-3} shown in Fig. 9.

changed from 2 dB to 6 dB.

5.2 Simulation Results

Figure 9 plots blocking ratios as a function of the total number of average path requests and a breakdown (% ratios) of each assigned modulation order/channel bandwidth in each network. In Scenario A, 16QAM signals cannot be assigned due to the large margin required. Scenario B and C can utilize 16QAM signals because the margin can be small thanks to the use of OPM. Moreover, Scenario C can further reduce the channel bandwidth thanks to adaptive bandwidth allocation. The proposed scheme thus can attain the highest spectral efficiency.

With regard to resource fragmentation, the T-F method can substantially increase the number of accommodated paths. In Scenario C, the T-F method outperforms the F-F method; the number of paths accommodated at the target blocking ratio of 10-3 is increased by 0–17.7% for British telecom, 0–19.4% for Telefonica, 0–18.6% for Phoenix, and 0–24.3% for 6×6 depending on the actually required margin. Note that no improvement is observed when the actually required margin is 6 dB. This is because only the QPSK signal with the 150-GHz bandwidth can be utilized due to the large margin and hence fragmentation is insignificant.

Figure 10 illustrates the number of accommodated paths at the blocking ratio of 10^{-3} as a function of actually required margin, where the results are estimated from Fig. 9. Compared to Scenario A, Scenario B with the T-F method can increase the number of accommodated paths by 0–94.6% for British telecom, 0–91.7% for Telefonica, 0–82.4% for Phoenix, and 0–77.6% for 6 × 6 depending on the actually required margin; Scenario C, our proposal, can increase the number of accommodated paths by 13.0–108% for British telecom, 11.8–106% for Telefonica, 10.6–88.4% for Phoenix, and 9.9–87.9% for 6 × 6.

6. Conclusion

In this paper, we discussed the effectiveness of transmission-quality-aware online network design and provisioning made possible by the built-in-receiver OPM based on Q-factor measurement; it offers adaptive control of modulation order and channel bandwidth for each path in highly dense WDM networks. The proposed control scheme can substantially reduce the margin normally needed to offset uncertain transmission impairments and system disaggregation and as a result the spectral efficiency of the network can be substantially improved. The effectiveness was confirmed by transmission experiments and network analyses. The spectral efficiency was increased by 9.9–108% compared to conventional distance-adaptive networks. The unallocated margin can be further reduced by increasing the numbers of modulation formats and channel bandwidths that can be selected, e.g. using probabilistic shaping or multi-dimensional modulation [21], [22].

Acknowledgments

This work was supported in part by NICT.

References

[1] M. Jinno, B. Kozicki, H. Takara, A. Watanabe, Y. Sone, T. Tanaka, and A. Hirano, “Distance-adaptive spectrum resource allocation in spectrum-sliced elastic optical path network,” IEEE Commun. Mag., vol.48, no.8, pp.138–145, 2010.

[2] N. Sambo, P. Castoldi, A. D’Errico, E. Riccardi, A. Pagano, M.S. Moreolo, J.M. Fàbrega, D. Rafique, A. Napoli, S. Frigerio, E.H. Salas, G. Zervas, M. Nolle, J.K. Fischer, A. Lord, and J.P.F.-P. Giménez, “Next generation sliceable bandwidth variable transponders,” IEEE Commun. Mag., vol.53, no.2, pp.163–171, 2015.

[3] T. Rahman, D. Rafique, B. Spinnler, S. Calabrò, E. Man, U. Feiste, A. Napoli, M. Bohn, G. Khanna, N. Hanik, E. Pincemin, C.L. Bouëtté, J. Jauffrit, S. Bordais, C. André, C. Dourthe, B. Raguénès, C.M. Okonkwo, A.M.J. Koonen, and H. Waardt, “Long-haul transmission of PM-16QAM-, PM-32QAM-, and PM-64QAM-based terabit superchannels over a field deployed legacy fiber,” IEEE/OSA J. Lightwave Technol., vol.34, no.13, pp.3071–3079, 2016.

[4] G. Bosco, V. Curri, A. Carena, P. Poggiolini, and F. Forghieri, “On the performance of Nyquist-WDM terabit superchannels based on PM-BPSK, PM-QPSK, PM-8QAM or PM-16QAM subcarriers,” OSA/IEEE J. Lightwave Technol., vol.29, no.1, pp.53–61, 2011.

[5] Y. Terada, Y. Mori, H. Hasegawa, and K. Sato, “Highly spectral efficient networks based on grouped optical path routing,” OSA Opt. Express, vol.24, no.6, pp.6213–6228, 2016.
[6] Y. Pointurier, “Design of low-margin optical networks,” IEEE/OSA J. Opt. Commun. Netw., vol.9, no.1, pp.A9–A17, 2017.
[7] M.P. Belanger, M. O’Sullivan, and P. Littlewood, “Margin requirement of disaggregating the DWDM transport system and its consequence on application,” OSA OFC 2018, paper M1E.2, 2018.
[8] N. Robinson, “Design and development of optical white box,” OSA OFC 2018, paper Tu3E.6, 2018.
[9] J. Slovak, W. Schairer, M. Herrmann, K. Pulverer, and E. Torrengo, “Benefits of performance awareness in coherent dynamic optical networks,” OSA OFC 2018, paper W4A.1, 2018.
[10] S. Oda, M. Miyabe, S. Yoshida, T. Katagiri, Y. Aoki, T. Hoshida, J.C. Rasmussen, M. Birk, and K. Tse, “A learning living network with open ROADMs,” OSA/IEEE J. Lightwave Technol., vol.35, no.8, pp.1350–1356, 2017.
[11] K. Kayano, Y. Mori, H. Hasegawa, K. Sato, S. Oda, S. Yoshida, and T. Hoshida, “Effectiveness of transmission-quality-aware online network design and provisioning enabled through optical performance monitoring,” IEICE Commun. Express, vol.8, no.4, pp.81–86, 2019.
[12] A.E. Willner, Z. Pan, and C. Yu, “Optical performance monitoring” Optical Fiber Telecommunications V B, I.P. Kaminow, T. Li, and A.E. Willner, eds., Chap. 27, Elsevier, 2008.
[13] C. Zhu, An V. Tran, S. Chen, L.B. Du, C.C. Do, T. Anderson, A.J. Lowery, and E. Skafidas, “Statistical moments-based OSNR monitoring for coherent optical systems,” OSA Opt. Express, vol.20, no.16, pp.17711–17721, 2012.
[14] Z. Dong, A.P.T. Lau, and C. Lu, “OSNR monitoring for QPSK and 16-QAM systems in presence of fiber nonlinearities for digital coherent receivers,” OSA Opt. Express, vol.20, no.17, pp.19520–19534, 2012.
[15] M.S. Faruk, Y. Mori, and K. Kikuchi, “In-band estimation of optical signal-to-noise ratio from equalized signals in digital coherent receivers,” IEEE Photonics J., vol.6, no.1, #7800109, 2014.
[16] Z. Shen, T. Kusano, H. Hasegawa, and K. Sato, “A novel routing and frequency slot assignment scheme that can adapt to transmission speed migration,” OSA OFC 2015, W1I.2, 2015.
[17] B.C. Chatterjee, S. Ba, and E. Oki, “Fragmentation problems and management approaches in elastic optical networks: A survey,” IEEE Commun. Surveys Tuts., vol.20, no.1, pp.183–210, 2018.
[18] Optical Internetworking Forum, “Technology options for 400G implementation,” OIF-Tech-Options-400G-01.0, 2015.
[19] ITU-T, “Spectral grids for WDM applications: DWDM frequency grid,” 2012.
[20] D. Chang, F. Yu, Z. Xiao, N. Stojanovic, F.N. Hauske, Y. Cai, C. Xie, L. Li, X. Xu, Q. Xiong, “LDPC convolutional codes using layered decoding algorithm for high speed coherent optical transmission,” OSA OFC 2012, OW1H.4, 2012.
[21] F.P. Guiomar, R. Li, C.R.S. Fludger, A. Carena, and V. Curri, “Hybrid modulation formats enabling elastic fixed-grid optical networks,” IEEE/OSA J. Opt. Commu. Netw., vol.8, no.7, pp.A92–A100, 2016.
[22] D.S. Millar, T. Koike-Akino, S.Ö. Arık, K. Kojima, K. Parsons, T. Yoshida, and T. Sugihara, “High-dimensional modulation for coherent optical communications systems,” vol.22, no.7, pp.8798–8812, 2014.

Keisuke Kayano received the B.E. degree and M.E. degree from Nagoya University in 2017 and 2019 respectively. His research interest includes optical networking, especially photonics network architecture and network design.

Yojiro Mori received the Ph.D. degree in engineering from the University of Tokyo, Japan, in 2013. He is currently an Assistant Professor at Nagoya University. Before joining the university, he was a Research Fellow of the Japan Society for the Promotion of Science from 2011 to 2012. In 2013, he joined the Department of Electrical Engineering and Computer Science at Nagoya University. His current research interests include digital coherent technologies and optoelectronic devices for photonic networks. Dr. Mori is a member of the Institute of Electronics, Information and Communication Engineers (IEICE) of Japan.

Hiroshi Hasegawa received his B.E., M.E., and D.E. degrees, all in electrical and electronic engineering, from Tokyo Institute of Technology in 1995, 1997, and 2000, respectively. He is currently a Professor at the Graduate School of Engineering of Nagoya University where he was an Associate Professor from 2005 to 2019. Before joining Nagoya University, he was an Assistant Professor at Tokyo Institute of Technology from 2000 to 2005. His current research interests include network/node architectures, devices, and design and control of photonic networks, multidimensional digital signal processing, and time-frequency analysis. Dr. Hasegawa is a senior member of IEICE and a member of IEEE.

Ken-ichi Sato received his B.S., M.S., and Ph.D. degrees in electronics engineering from the University of Tokyo, in 1976, 1978, and 1986, respectively. He is a Professor Emeritus at the Graduate School of Engineering, Nagoya University, an NTT R&D Fellow, and currently with Advanced Industrial Science and Technology (AIST). Before joining the university in April 2004, he was an Executive Manager of the Photonic Transport Network Laboratory at NTT. He has been a leading researcher in the field of telecommunications; his most significant achievements lie in two of the important transport network technology developments. One is ATM (Asynchronous Transfer Mode) network technology, which includes the invention of the Virtual Path concept. The other is photonic network technology, which includes the invention of the optical path concept and various networking and system technologies. His R&D activities cover transport network architectures, network design, photonic network systems including optical cross-connect/ADM and photonic IP routers, and optical transmission technologies. He has authored/co-authored more than 500 research publications in international journals and conferences. He holds 50 granted patents and more than 100 pending patents. His contributions to asynchronous transfer mode (ATM) and optical network technology development extend to coediting the IEEE Journal on Selected Areas in Communications (four special issues) and the Journal of Lightwave Technology (three special issues); organizing several workshops and conference technical sessions; serving on numerous committees of international conferences including OFC 2016 General Chair and OFC 2014 Program Chair; authoring a book, Advances in Transport Network Technologies (Artech House, 1996); and coauthoring 14 other books. Prof. Sato is a Fellow of the Institute of Electronics, Information and Communication Engineers (IEICE) of Japan and a Fellow of the IEEE. He served as the president of the IEICE during 2016–2017. He received the Young Engineer Award in 1984, the Excellent Paper Award in 1991, the Achievement Award in 2000, and the Distinguished Achievement and Contributions Award in 2011 from the IEICE of Japan, and the Best Paper Awards in 2007 and 2008 from the IEICE Communications Society. He was also the recipient of the Distinguished Achievement Award of the Ministry of Education, Science and Culture in 2002, and the Medal of Honor with Purple Ribbon from Japan's Cabinet Office in 2014.

Shoichiro Oda received B.E., M.E., and Ph.D. degrees in electronic, information systems, and energy engineering from Osaka University, Suita, Japan, in 2002, 2003, and 2006, respectively. From 2006 to 2007, he was a postdoctoral researcher with the Chalmers Technology of University, Gothenburg, Sweden, where his research interests included fiber-optic parametric amplifiers and their applications. In 2007, he joined Fujitsu Laboratories Ltd., Kawasaki, Japan. Since 2011, he has been with Fujitsu Limited, Kawasaki, Japan where he is involved in the research and development of wavelength-division multiplexing transmission systems. He is a member of Institute of Electronics, Information and Communication Engineers (IEICE) of Japan.

Setsuo Yoshida received the B.S. and M.S. degrees from Hokkaido University, Sapporo, Japan, in 1993 and 1995, respectively. In 2000, he joined Fujitsu Laboratories Ltd., Kawasaki, Japan. Since 2005, he has been with Fujitsu Limited, Kawasaki, Japan, where he has been engaged in research and development of controlling technology of optical device. He is a member of the Institute of Electronics, Information, and Communication Engineers (IEICE) of Japan.

Takeshi Hoshida received B.E., M.E., and Ph.D. degrees in electronic engineering from the University of Tokyo, Tokyo, Japan, in 1993, 1995, and 1998, respectively. Since 1998, he has been with Fujitsu Laboratories Ltd., Kawasaki, Japan, where he has been engaged in the research and development of dense wavelength-division multiplexing optical transmission systems. From 2000 to 2002, he was with Fujitsu Network Communications, Inc., Richardson, Texas. Since 2007, he has also been with Fujitsu Limited, Kawasaki, Japan. He is a senior member of the Institute of Electronics, Information and Communication Engineers (IEICE) and a member of the Japan Society of Applied Physics (JSAP).